Continuous fat oxidation in acetyl–CoA carboxylase 2 knockout mice increases total energy expenditure, reduces fat mass, and improves insulin sensitivity

Cheol Soo Choi*, David B. Savage*, Lutfi Abu-Elheiga†, Zhen-Xiang Liu*, Sheene Kim*, Ameya Kulkarni*, Alberto Distefano*, Yu-Jin Hwang*, Richard M. Reznick*, Roberto Codella*, Dongyan Zhang*, Gary W. Cline*, Salih J. Wakil†‡, and Gerald I. Shulman*§¶‖

Departments of *Internal Medicine and §Cellular and Molecular Physiology and ¶Howard Hughes Medical Institute, Yale University School of Medicine, New Haven, CT 06510; and †Verna and Marrs McLean Department of Biochemistry and Molecular Biology, Baylor College of Medicine, One Baylor Plaza, Houston, TX 77030

Contributed by Salih J. Wakil, July 30, 2007 (sent for review June 1, 2007)

Acetyl–CoA carboxylase 2 (ACC)2 is a key regulator of mitochondrial fat oxidation. To examine the impact of ACC2 deletion on whole-body energy metabolism, we measured changes in substrate oxidation and total energy expenditure in *Acc2*$^{-/-}$ and WT control mice fed either regular or high-fat diets. To determine insulin action *in vivo*, we also measured whole-body insulin-stimulated liver and muscle glucose metabolism during a hyperinsulinemic–euglycemic clamp in *Acc2*$^{-/-}$ and WT control mice fed a high-fat diet. Contrary to previous studies that have suggested that increased fat oxidation might result in lower glucose oxidation, both fat and carbohydrate oxidation were simultaneously increased in *Acc2*$^{-/-}$ mice. This increase in both fat and carbohydrate oxidation resulted in an increase in total energy expenditure, reductions in fat and lean body mass and prevention from diet-induced obesity. Furthermore, *Acc2*$^{-/-}$ mice were protected from fat-induced peripheral and hepatic insulin resistance. These improvements in insulin-stimulated glucose metabolism were associated with reduced diacylglycerol content in muscle and liver, decreased PKCθ activity in muscle and PKCε activity in liver, and increased insulin-stimulated Akt2 activity in these tissues. Taken together with previous work demonstrating that *Acc2*$^{-/-}$ mice have a normal lifespan, these data suggest that *Acc2* inhibition is a viable therapeutic option for the treatment of obesity and type 2 diabetes.

diet-induced obesity prevention | intracellular diacylglycerol | increased fat oxidation | insulin resistance prevention

Acetyl–CoA carboxylase (ACC) catalyses the synthesis of malonyl CoA, a precursor for fatty acid synthesis and an allosteric inhibitor of carnitine palmitoyltransferase 1 (1–3). The fact that carnitine palmitoyltransferase 1 regulates fatty acid transfer into mitochondria for subsequent oxidation means that ACC regulates both fatty acid synthesis and oxidation (1–4). There are two ACC isoforms. ACC1 is highly expressed in adipose tissue and liver and is essential for survival (5, 6). ACC2 is primarily expressed in oxidative tissues, such as heart and skeletal muscle, but is also expressed in liver, and adipose tissues (5). The regulation of ACC can be at the level of gene expression or by modulation of enzymatic activities either through allosteric regulation by citrate and palmitoyl–CoA or by phosphorylation/dephosphorylation of specific serine residues by both cAMP-dependent PKA and AMP-activated PK (AMPK) (7–11).

Acc2 knockout (*Acc2*$^{-/-}$) mice are viable but leaner than WT controls, and *ex vivo* measurements of fat oxidation in muscle and fat obtained from *Acc2*$^{-/-}$ mice have revealed increased rates of fat oxidation (12, 13). Given the potentially important role of intracellular fatty acid metabolites in mediating insulin resistance in liver and skeletal muscle (14–17), one would predict that *Acc2*$^{-/-}$ mice should be protected from fat-induced insulin resistance. However, the Randle hypothesis states that fat oxidation and carbohydrate oxidation are mutually inhibitory (18, 19). Because insulin-induced changes in ACC activity are pivotal in switching between carbohydrate and fat oxidation during the fed-fasting transition, knocking out *Acc2*, according to this model, would result in higher fat oxidation and lower glucose oxidation, regardless of the nutritional state leading to insulin resistance. Therefore, the aim of this study was to examine each of these hypotheses by evaluating whole-body insulin action in *Acc2*$^{-/-}$ mice by the hyperinsulinemic–euglycemic clamp in combination with detailed analyses of insulin signaling in liver and muscle. In addition, we sought to examine the impact of ACC2 deficiency on whole-body energy expenditure, activity, and food intake in *Acc2*$^{-/-}$ mice fed either a regular chow diet or a high-fat diet (HFD).

Results

Fat Mass Was Reduced Secondary to Increased Energy Expenditure in *Acc2*$^{-/-}$ Mice. Total body weights were significantly reduced in *Acc2*$^{-/-}$ mice fed either a regular diet or HFD despite increased food consumption (Table 1). NMR analysis of body composition suggested that this was a result of a reduction in both fat and lean body mass (Table 1). High-fat feeding (3 weeks) increased body weight in WT littermates to a greater extent than in *Acc2*$^{-/-}$ mice (3.6 ± 0.4 g vs. 2.0 ± 0.4 g; $P = 0.02$), the difference being exclusively attributable to greater fat gain (WT vs. *Acc2*$^{-/-}$ mice: 3.62 ± 0.4 g vs. 2.4 ± 0.5 g; $P = 0.05$). To evaluate the prevention of HFD-induced obesity in *Acc2*$^{-/-}$ mice, energy balance of the mice was assessed in an animal metabolic monitoring system for 4 days (2 days of acclimation followed by 2 days of measurements). Although locomotor activity was similar in the WT and *Acc2*$^{-/-}$ mice, total energy expenditure was 15 and 19% higher in *Acc2*$^{-/-}$ mice fed the regular diet or HFD, respectively (Fig. 1 *A* and *B* and Table 1). As we reported previously (5), there was a significant increase in food intake in *Acc2*$^{-/-}$ mice compared with the WT. These results are consistent with the role of malonyl–CoA in regulating food intake in mice (20).

Substrate Selection in *Acc2*$^{-/-}$ Mice. Because knocking out ACC2 would be expected to promote fat oxidation regardless of the

Author contributions: C.S.C. and D.B.S. contributed equally to this work; C.S.C., D.B.S., L.A.-E., S.J.W., and G.I.S. designed research; C.S.C., Z.-X.L., S.K., A.K., A.D., Y.-J.H., R.M.R., and D.Z. performed research; C.S.C., D.B.S., L.A.-E., Z.-X.L., S.K., A.K., A.D., Y.-J.H., R.M.R., R.C., D.Z., G.W.C., S.J.W., and G.I.S. analyzed data; and C.S.C., D.B.S., L.A.-E., Z.-X.L., S.K., A.K., A.D., Y.-J.H., R.M.R., R.C., D.Z., G.W.C., S.J.W., and G.I.S. wrote the paper.

The authors declare no conflict of interest.

Abbreviations: ACC, acetyl–CoA carboxylase; AMPK, AMP-activated PK; HFD, high-fat diet; nPKC, novel PKC; RQ, respiratory quotient.

‡To whom correspondence may be addressed. E-mail: swakil@bcm.tmc.edu.

‖To whom correspondence may be addressed at: Yale University School of Medicine, TAC S269, P.O. Box 9812, New Haven, CT 06536-8012. E-mail: gerald.shulman@yale.edu.

Table 1. Basal metabolic parameters of energy balance

	Regular diet		HFD	
Metabolic parameter	WT ($n = 11$)	$Acc2^{-/-}$ ($n = 10$)	WT ($n = 10$)	$Acc2^{-/-}$ ($n = 10$)
Body weight, g	30.5 ± 0.3	26.2 ± 0.5*	34.1 ± 0.4	28.2 ± 0.8*
Fat mass, g	2.86 ± 0.27	2.24 ± 0.26	6.37 ± 0.28	4.65 ± 0.37†
Lean body mass, g	22.9 ± 0.3	20.0 ± 0.5*	23.11 ± 0.32	19.67 ± 0.47*
Total energy expenditure	19.8 ± 0.4	23.5 ± 1.4‡	22.8 ± 0.6	26.0 ± 0.7‡
Food intake	23.8 ± 1.7	30.9 ± 1.3‡	25.5 ± 3.0	26.2 ± 2.2
Activity, counts	67.9 ± 9.7	84.1 ± 21.1	79.4 ± 5.3	75.7 ± 10.0
RQ	0.925 ± 0.013	0.933 ± 0.008	0.793 ± 0.007	0.798 ± 0.007

Total energy expenditure and food intake were measured in kilocalories (1 cal = 4.18 kJ) per hour per kilogram of lean body mass. *, $P < 0.001$; †, $P < 0.01$; ‡, $P < 0.05$ ($Acc2^{-/-}$ vs. WT).

nutritional state, we examined respiratory quotient (RQ) profiles, which reflect the relative contributions of carbohydrate and fat oxidation to total energy expenditure. Surprisingly, RQ was similar in regular-diet-fed (60% carbohydrate, 10% fat, 30% protein calories) $Acc2^{-/-}$ and WT mice during both the light (fasting) and dark (fed) phase (Fig. 1*C* and Table 1). Switching the mice from a regular diet to a HFD (24% carbohydrate, 55% fat, 21% protein calories) reduced RQ to the same extent in WT and $Acc2^{-/-}$ mice (Fig. 1*D*). Given the marked increase in total energy expenditure in $Acc2^{-/-}$ mice (Fig. 1*A*), the similar RQ profiles of both groups suggest that fat and carbohydrate oxidation were significantly increased in the $Acc2^{-/-}$. Plasma ketone concentrations, which reflect hepatic fat oxidation, were increased in $Acc2^{-/-}$ mice in both the fed and fasting state (Table 2). We also measured liver glycogen content in both states. After overnight fasting, liver glycogen stores were almost totally depleted in WT and $Acc2^{-/-}$ mice (data not shown). Five hours after refeeding, glycogen stores were replenished in both groups, but $Acc2^{-/-}$ mice stored less glycogen in the liver [WT ($n = 8$) vs. $Acc2^{-/-}$ mice ($n = 6$): 4.5 ± 0.24 vs. 3.0 ± 0.43 g per 100 g of liver; $P = 0.008$].

Hepatic and Peripheral Insulin Sensitivities Are Increased in High-Fat-Fed *Acc2*$^{-/-}$ Mice. Fasting plasma glucose and insulin concentrations were reduced by ≈30% in high-fat-fed $Acc2^{-/-}$ mice (Table 2) compared with high-fat-fed WT mice, whereas plasma fatty acids, triglycerides, and cholesterol were similar in both groups (Table 2). To gain further insight into insulin action on whole-body and tissue-specific glucose metabolism, we performed hyperinsulinemic–euglycemic clamps with radioisotope-labeled glucose infusion. Consistent with previous studies (21, 22), high-fat feeding induced severe liver (Fig. 2*C*) and muscle (Fig. 2*D*) insulin resistance in the WT mice. Insulin responsiveness in the $Acc2^{-/-}$ mice was markedly increased, as reflected by a 2-fold increase in the steady-state glucose infusion rate to maintain euglycemia during the hyperinsulinemic–euglycemic clamps (Fig. 2 *A* and *B*). This improvement in insulin-stimulated glucose metabolism in the $Acc2^{-/-}$ mice could be attributed to a 78% increase in insulin-induced suppression of hepatic glucose production (Fig. 2*C*) and a 42% increase in insulin-stimulated whole-body glucose uptake (Fig. 2*D*). The increase in whole-body glucose uptake was associated with significant increases in whole-body glycolysis (26%) and glycogen synthesis (75%) (Fig. 2*D*). Glucose uptake in skeletal muscle (SKM) and white adipose tissue were increased by 66% and 100%, respectively, in $Acc2^{-/-}$ mice (Figs. 2 *E* and *F*). The ability of insulin to suppress peripheral lipolysis and reduce fatty acid concentration, which serves as an index of adipose tissue insulin sensitivity, was also higher by 42% in $Acc2^{-/-}$ mice than the WT control mice during the hyperinsulinemic–euglycemic clamps (Fig. 2*G*). Although insulin was infused at a constant and identical rate throughout the clamp studies, plasma insulin concentrations were 26% lower in the $Acc2^{-/-}$ mice, suggesting increased insulin clearance (Table 2).

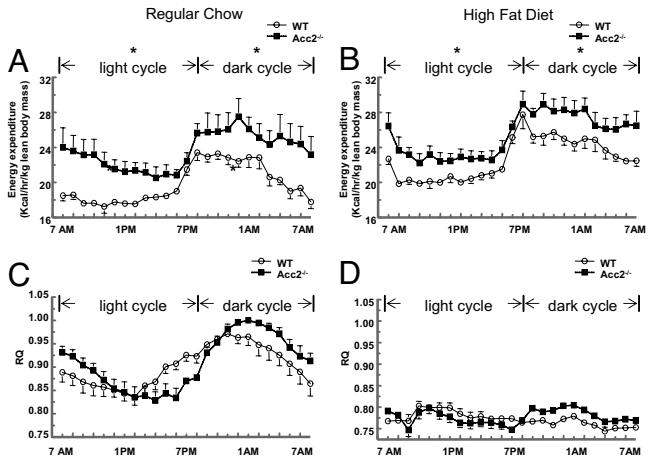

Fig. 1. Energy balance and substrate selection. Energy expenditure (*A* and *B*) and RQ (*C* and *D*) were assessed by a comprehensive animal metabolic monitoring system (CLAMS) in $Acc2^{-/-}$ and WT mice fed a regular diet and a HFD. Metabolic parameters were measured over a 48-h period, and equivalent time points, which were collected during the first and second 24-h periods, were averaged together. The results are a profile of the average energy expenditure of each group per hour during the 24-h course. The data are expressed as mean values ± SEM of five to eight mice per group. *, $P < 0.05$ ($Acc2^{-/-}$ vs. WT).

Decreased Novel PKC Membrane Translocation and Increased Akt2 Activity in *Acc2*$^{-/-}$ Mice. Previously, we have implicated increased novel (n)PKC activity in muscle (PKCθ) and liver (PKCε) in mediating fat-induced insulin resistance in these tissues (17, 23–28). Consistent with this hypothesis, improved insulin sensitivity in muscle and liver of high-fat-fed $Acc2^{-/-}$ mice was associated with a 30–40% reduction in the membrane translocation of PKCθ and PKCε in muscle and liver, respectively (Fig. 3 *A* and *B*), and a 30–40% increase in insulin-stimulated Akt2 activity (Fig. 3 *C* and *D*).

Decreased Triglycerides, Diacylglycerol, and Long-Chain Acyl–CoAs but Not Ceramide in *Acc2*$^{-/-}$ Mice. Intracellular concentrations of triglyceride and long-chain acyl–CoAs were lower in the liver and skeletal muscle of $Acc^{-/-}$ mice compared with WT mice (Fig. 4 *A*, *B*, *E*, and *F*). More importantly, the concentrations of diacylglycerol in liver and the membrane/cytosol ratio of skeletal muscle diacylglycerol were decreased by ≈50% in the high-fat-fed $Acc2^{-/-}$ mice compared with the high-fat-fed WT mice (Figs. 4 *C* and *D*). Ceramides have also been suggested to be mediators of insulin resistance (29, 30). In contrast to the observed difference in diacylglycerol, there was no difference in ceramide content of

BIOCHEMISTRY

Table 2. Plasma metabolite, hormone, and cytokine data from high-fat-fed WT and *Acc2*$^{-/-}$ mice

	Fast		Clamp		Fed	
Parameter	WT ($n = 9$)	*Acc2*$^{-/-}$ ($n = 9$)	WT ($n = 9$)	*Acc2*$^{-/-}$ ($n = 9$)	WT ($n = 8$)	*Acc2*$^{-/-}$ ($n = 6$)
Glucose, mg/dl	131 ± 8	96 ± 8*	118 ± 2	124 ± 3	214 ± 6	189 ± 12
Insulin, microunits/ml	16.6 ± 1.2	11.7 ± 1.0*	77.9 ± 3.3	57.4 ± 6.4†	ND	ND
Fatty acids, mEq/liter	1.05 ± 0.11	1.15 ± 0.05	0.74 ± 0.08	0.43 ± 0.06*	0.45 ± 0.04	0.46 ± 0.05
Triglycerides, mg/dl	115 ± 15	113 ± 8	ND	ND	107 ± 18	99 ± 5
Cholesterol, mg/dl	100 ± 10	109 ± 7	ND	ND	116 ± 13	105 ± 13
β-Hydroxybutyrate, mM	1.76 ± 0.13	2.83 ± 0.35*	ND	ND	0.26 ± 0.03	0.48 ± 0.11†
Resistin, pM	1,607 ± 333	1,498 ± 172				
TNF-α, pM	2.31 ± 0.25	3.19 ± 0.67				
IL-6, pM	4.75 ± 0.81	6.25 ± 1.86				
Leptin, pM	3,499 ± 1,627	2,869 ± 981				
Adiponectin, μg/ml	7.5 ± 1.6	9.3 ± 1.8				

*, $P < 0.01$; †, $P < 0.05$ (*Acc2*$^{-/-}$ vs. WT); ND, not determined.

skeletal muscle between WT and *Acc2*$^{-/-}$ mice [WT ($n = 8$) vs. *Acc2*$^{-/-}$ mice ($n = 5$): 51.1 ± 3.5 vs. 55.4 ± 4.2 nmol/g, $P = 0.45$].

Plasma Adipocytokines and AMPK-α_2 Activity in Skeletal Muscle. Recent studies have suggested that circulating adipocytokines can modulate insulin sensitivity and fat content of liver and muscle (31–34). Thus we measured plasma concentrations of resistin, TNFα, IL-6, leptin, and adiponectin but found no significant differences in plasma concentrations of these adipocytokines between *Acc2*$^{-/-}$ and WT mice (Table 2). In addition, because an increase in AMPK activity could also explain many of the observations in *Acc2*$^{-/-}$ mice, we also measured AMPK-α_2 activity in the *Acc2*$^{-/-}$ and WT mice. However, there was no difference in AMPK-α_2 activity in the tibialis anterior (TA), a mixed fiber-type muscle, between the two groups [WT, 0.75 ± 0.14 ($n = 9$) vs. *Acc2*$^{-/-}$ 0.45 ± 0.10 pmol/min·mg^{-1} ($n = 8$); P, not significant].

Discussion

Recent studies have strongly implicated increases in intracellular lipid content in liver and skeletal muscle because of increased fatty acid delivery and/or decreased fat oxidation in causing insulin resistance in these tissues (17). This hypothesis has generated interest in potential therapeutic strategies aimed at increasing mitochondrial fat oxidation to decrease the intracellular lipid contents. By controlling malonyl–CoA levels at the mitochondrial carnitine palmitoyltransferase 1, ACC2 regulates fatty acid transfer into mitochondria where they are subsequently oxidized. Previous studies have demonstrated that knocking out *Acc2* in mice results in significant increases of fat oxidation in fat, muscle, and liver *in vitro* (12, 13). In this study, we assessed body composition and energy balance in these mice and found that fat and lean mass were reduced in *Acc2*$^{-/-}$ mice and that this could be attributed to 19 and 14% increases in whole-body energy expenditure in *Acc2*$^{-/-}$ mice fed either a regular diet or HFD, respectively (Table 1). The fact that energy expenditure was increased throughout the light and dark cycle and that physical activity was similar in WT and *Acc2*$^{-/-}$ mice suggests that substrate oxidation is continuously higher in the *Acc2*$^{-/-}$ mice. Fat oxidation and carbohydrate oxidation are thought to be mutually inhibitory; in fact, this competition was a key element in the Randle hypothesis, which originally offered an attractive explanation for fatty acid-induced insulin resistance (18, 19). However, we observed identical RQ measurements throughout the light and dark cycle, despite higher energy expenditure in the *Acc2*$^{-/-}$ mice, suggesting that knocking out *Acc2* increased carbohydrate oxidation to the same extent as fat oxidation. This observation is supported by the increase in glucose and fat oxidation noted previously in adipocytes obtained from *Acc2*$^{-/-}$ mice (13). Taken together, these data suggest that there is a simultaneous increase in both glucose and fatty acid oxidation rather than fuel competition between fat and carbohydrate in *Acc2*$^{-/-}$ mice.

Although protection from diet-induced obesity is clearly beneficial, the loss of lean body mass and increased fatty acid oxidation, as seen in *Acc2*$^{-/-}$ mice, may not be beneficial in terms of insulin sensitivity, raising concerns about the metabolic consequences of ACC2 inhibition. To address this, we performed hyperinsulinemic–euglycemic clamps in high-fat fed *Acc2*$^{-/-}$ mice and WT littermates to assess hepatic and peripheral insulin sensitivity. As in our previous studies (21, 22), high-fat feeding induced severe insulin resistance in the WT mice, as reflected by lack of suppression of hepatic glucose production and markedly decreased peripheral glucose uptake during the clamp under physiological insulin levels. In contrast, insulin responsiveness in both liver and peripheral tissues was improved in *Acc2*$^{-/-}$ mice compared with the WT mice. Notably, insulin-stimulated glucose uptake was increased in skeletal muscle, where ACC2 is most highly expressed, and its deficiency induces fat oxidation. In keeping with the idea that fuel competition is not operating in the *Acc2*$^{-/-}$ mice, tissue insulin sensitivity was improved rather than inhibited despite increased fat oxidation. Whole-body glycolysis, which accounts for the majority of insulin-stimulated glucose disposal in mice, was increased by 26%, and glycogen synthesis was increased by 75%. Although the latter data suggest that glucose was preferentially stored as glycogen in *Acc2*$^{-/-}$ mice, the absolute changes in glycolytic flux and glycogen synthesis flux were similar (5.9 vs. 7.4 mg/kg·min^{-1}). These changes in whole-body insulin-stimulated glucose flux were accompanied by concordant improvements in insulin signaling in liver and muscle tissue. Fasting plasma concentrations of fatty acids, triglyceride, and cholesterol were similar in both groups; this observation may reflect increased flux of lipids from adipose tissue to liver and other oxidative tissues. HFD-induced or obesity-related insulin resistance is usually accompanied by impaired insulin clearance (35–37), and weight loss enhances insulin clearance (35, 38). Consistent with these findings, we observed lower plasma insulin concentrations in *Acc2*$^{-/-}$ mice during the hyperinsulinemic–euglycemic clamp.

The above data strongly suggest that ectopic lipid accumulation causes insulin resistance and that increased fat oxidation improves insulin sensitivity. However, the molecular mechanisms responsible for this relationship remain uncertain. We have suggested that fat-induced insulin resistance in muscle and liver is caused by intracellular accumulation of diacylglycerol, which activates PKCθ in muscle and PKCε in liver, which, in turn, activate a serine kinase cascade that leads to impaired insulin signaling in these tissues (17, 23–28, 39). We therefore predicted that any metabolic change that reduces the accumulation of intracellular fatty acid metabolites and, in particular, diacylglycerol (a potent activator of nPKCs) might result in amelioration of insulin resistance in liver and skeletal muscle (17). Consistent with this hypothesis, we found that knock-

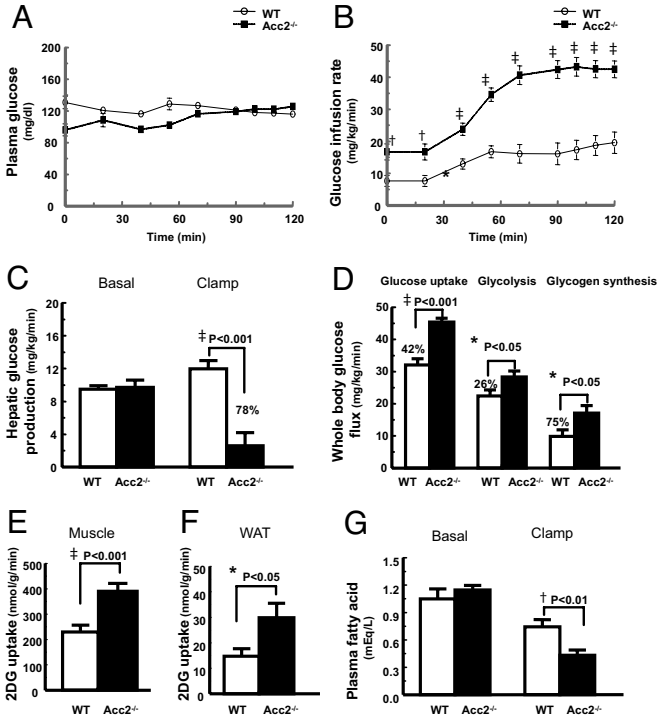

Fig. 2. Knocking out of ACC2 significantly improved hepatic and peripheral insulin sensitivity in high-fat-fed mice. Peripheral and hepatic insulin sensitivity was assessed by means of hyperinsulinemic–euglycemic clamps. (*A*) Plasma glucose. (*B*) Glucose infusion rates. (*C*) Hepatic glucose production during hyperinsulinemic–euglycemic clamps. (*D*) Whole-body glucose uptake, whole-body glycolysis, and whole-body glycogen synthesis. (*E*) Skeletal muscle (gastrocnemius) glucose uptake. (*F*) Epididymal white adipose tissue (WAT) glucose uptake. (*G*) Suppression of plasma fatty acid concentrations during the clamps. The data are expressed as mean values ± SEM for nine mice per group. *, $P < 0.05$; †, $P < 0.01$; ‡, $P < 0.001$ (*Acc2* $^{-/-}$ vs. WT); 2DG, 2-deoxy glucose.

ing out ACC2 increased whole-body fat oxidation, resulting in a ≈50% reduction in diacylglycerol content in liver and in the membrane-to-cytosol ratio of diacylglycerol in skeletal muscle. These changes were also associated with decreased PKCε activity in liver and PKCθ activity in skeletal muscle and increased insulin-stimulated AKT activity in these tissues. Furthermore, these changes were not associated with any changes in plasma concentrations of IL-6, TNF-α, adiponectin, or resistin, suggesting that these adipocytokines were not involved in mediating insulin resistance in this mouse model.

Several pharmacological attempts have been made to inhibit ACC (40). Major difficulties have included problems in generating ACC isoform specific inhibitors. The ACC1 knockout is embryonic lethal, suggesting that ACC2 is a better therapeutic target than ACC1. Although we have effectively used isoform specific antisense oligonucleotide inhibitors or combinations thereof in a rat model of nonalcoholic fatty liver disease, target knockdown was confined to liver and fat, leaving ACC2 in muscle unchanged (28). Because muscle is a major oxidative tissue, this likely explains why we did not observe any similar reductions in body weight in the ACC1/ACC2 antisense oligonucleotide inhibitor studies (28). The data presented suggest that further attempts to target ACC2 in at least fat, muscle, and liver are warranted.

In summary, we have shown that constitutively promoting fat oxidation by knocking out *Acc2* increases energy expenditure and reduces fat and lean mass in mice. Reassuringly, these changes are associated with improved peripheral and hepatic insulin sensitivity. These data suggest that ACC2 inhibitors remain a potentially useful therapeutic option for treatment of obesity and type 2 diabetes.

Materials and Methods

Animals. *Acc2*$^{-/-}$ mice were generated as described previously (5). Mice were housed under controlled temperature (22 ± 2°C) and lighting (12 h of light, 0700–1700 hours; 12 h of dark, 1700–0700 hours) with free access to water and food. To examine the diet-induced changes in glucose and fat metabolism, male *Acc2*$^{-/-}$ and WT mice were fed a regular diet (TD2018; Harlan Teklad, Madison, WI) or HFD (55% fat by calories; TD 93075; Harlan Teklad) ad libitum at the age of 17–18 weeks for 3 weeks, and metabolic parameters and insulin action were measured. Mice were maintained in accordance with the Institutional Animal Care and Use Committee of the Yale University School of Medicine.

Basal Study. Fat and lean body masses were assessed by ^{1}H magnetic resonance spectroscopy (Bruker BioSpin, Billerica, MA) before and after 3 weeks of high-fat feeding. A comprehensive animal metabolic monitoring system (CLAMS; Columbus Instruments, Columbus, OH) was also used to evaluate activity, food consumption, and energy expenditure before and after 3 weeks of high-fat feeding. Energy expenditure and food intake data were normalized with respect to lean body weight. Energy expenditure and RQ were calculated from the gas exchange data [energy expenditure = $(3.815 + 1.232 \times \mathrm{RQ}) \times \mathrm{VO_2}$]. RQ is the ratio of $\mathrm{VCO_2}$ to $\mathrm{VO_2}$, which changes depending on the energy source the animal is using. When carbohydrates are the only substrate being oxidized, the RQ will be 1.0, and it will be 0.7 when only fatty acids are oxidized. Activity was measured on *x* and *z* axis by using infrared beams to count the beam breaks during a specified measurement period. Feeding is measured by recording the difference in the scale measurement of the center feeder from one time point to another. We studied five to eight male mice per group. Additional blood samples were obtained for the measurement of plasma lipid and ketone body concentrations at the overnight fasting states.

Hyperinsulinemic–Euglycemic Clamp Study. Seven days before the hyperinsulinemic–euglycemic clamp studies, indwelling catheters were placed into the right internal jugular vein extending to the right atrium. After an overnight fast, [3-^{3}H]glucose (HPLC purified; PerkinElmer, Boston, MA) was infused at a rate of 0.05 μCi/min for basal 2 h to assess the basal glucose turnover. After the basal period, hyperinsulinemic–euglycemic clamp was conducted for 120 min with a primed/continuous infusion of human insulin (126 pmol/kg, prime; 18 pmol/kg·min^{-1}, infusion) (Novo Nordisk, Princeton, NJ) to raise plasma insulin within the physiological range. Blood samples (10 μl) were collected at 10- to 20-min intervals for immediate measurement of plasma glucose, and 20% dextrose was infused at various rates to maintain plasma glucose at basal concentrations (≈6.7 mM). To estimate insulin-stimulated whole-body glucose fluxes, [3-^{3}H]glucose was infused at a rate of 0.1 μCi/min throughout the clamps and 2-deoxy-D-[1-^{14}C]glucose (PerkinElmer) was injected as a bolus at minute 75 of the clamp to estimate the rate of insulin-stimulated tissue glucose uptake, as described previously (22). Blood samples (10 μl) for the measurement of plasma ^{3}H and ^{14}C activities were taken at the end of the basal period and during the last 45 min of the clamp. Additional blood samples were obtained for the measurement of plasma insulin and free fatty acid concentrations at the end of basal and clamp periods. At the end of the clamp, mice were anesthetized with pentobarbital sodium injection and tissues were taken for biochemical measurements within 4 min. Each tissue, once exposed, was dissected out within 2 sec, frozen immediately by using liquid N_2-cooled aluminum blocks, and stored at −80°C for subsequent analysis.

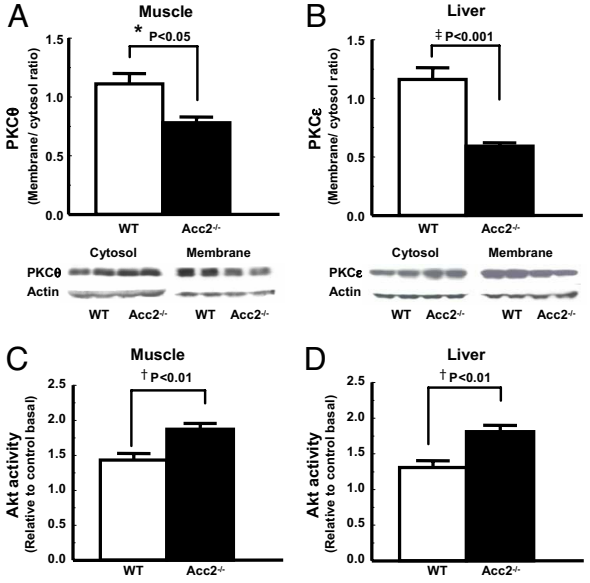

Fig. 3. Knocking out of *Acc2* increased Akt2 activity and decreased PKC membrane translocation. (*C* and *D*) Improved muscle and hepatic insulin sensitivity are associated with increased Akt2 activity in muscle (*C*) and liver (*D*). (*A* and *B*) Reduced membrane translocation of PKCθ in muscle (*A*) and PKCε in liver (*B*) may be directly involved in improving muscle and hepatic insulin signaling. Akt2 activity was assessed 14 min after i.p. insulin injection of 1 unit per kilogram of body weight. Data are expressed as mean values ± SEM for four to five mice per group. *, $P < 0.05$; †, $P < 0.01$; ‡, $P < 0.001$ (*Acc2* $^{-/-}$ vs. WT).

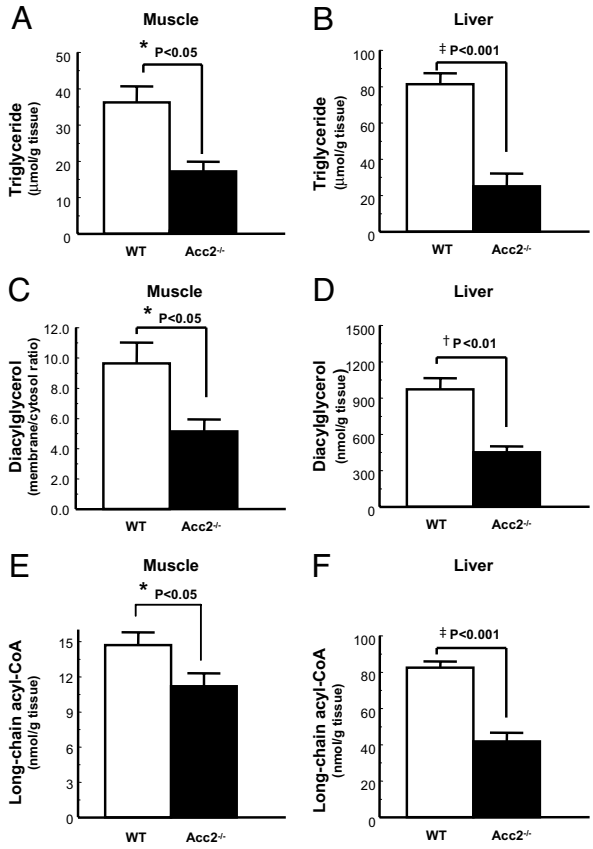

Fig. 4. Decreased triglycerides, diacylglycerol, and long-chain acyl–CoAs in *Acc2*$^{-/-}$ mice. (*A*, *B*, *E*, and *F*) Triglyceride and long-chain acyl–CoA levels were significantly decreased in muscle (*A* and *E*) and liver (*B* and *F*) in *Acc2*$^{-/-}$ mice. (*C* and *D*) Skeletal muscle membrane-to-cytosol ratio of diacylglycerols (*C*) and hepatic diacylglycerols (*D*) were significantly lower in *Acc2*$^{-/-}$ mice compared with WT mice. Data are expressed as mean values ± SEM for five to eight mice per group. *, $P < 0.05$, †, $P < 0.01$; ‡, $P < 0.001$ (*Acc2* $^{-/-}$ vs. WT).

Glucose Flux Calculation. For the determination of plasma ^{3}H-glucose, plasma was deproteinized with $ZnSO_4$ and $Ba(OH)_2$, dried to remove ^3H_2O, resuspended in water, and counted in scintillation fluid (Ultima Gold; PerkinElmer) on a scintillation counter (Beckman, Fullerton, CA). Rates of basal and insulin-stimulated whole-body glucose turnover were determined as the ratio of the [3-^{3}H]glucose infusion rate (dpm) to the specific activity of plasma glucose (dpm per milligram) at the end of the basal period and during the final 30 min of the clamp experiment, respectively. Hepatic glucose production was determined by subtracting the glucose infusion rate from the total glucose appearance rate.

The plasma concentration of ^3H_2O was determined by the difference between ^{3}H counts without and with drying. Whole-body glycolysis was calculated from the rate of increase in plasma ^3H_2O concentration divided by the specific activity of plasma ^{3}H-glucose, as described previously (41). Whole-body glycogen synthesis was estimated by subtracting whole-body glycolysis from whole-body glucose uptake, assuming that glycolysis and glycogen synthesis accounted for the majority of insulin-stimulated glucose uptake (42).

For the determination of individual tissue glucose uptake, tissue samples were homogenized and the supernatants were subjected to an ion-exchange column to separate tissue ^{14}C-2-deoxy glucose (^{14}C-2-DG)-6-phosphate from ^{14}C-2-DG. Tissue glucose uptake was calculated from the area under curve of plasma ^{14}C-2-DG profile and muscle ^{14}C-2-DG-6-phosphate content, as described previously (41).

Biochemical Analysis. Plasma glucose was analyzed during the clamps by using 10 μl of plasma by a glucose oxidase method on a Glucose Analyzer II (Beckman). Plasma insulin levels were determined by RIA by using a RIA kit from Linco Research (St. Louis, MO). Plasma FFA was determined by using an acyl–CoA oxidase based colorimetric kit (Wako Pure Chemical Industries, Osaka, Japan). Plasma resistin, leptin, TNFα, and IL-6 were measured by multiplexed biomarker immunoassays (Lincoplex), and adiponectin was measured by an RIA kit from Linco Research.

Insulin Signaling and PKCs. Akt2 activity was assessed in protein extracts from muscle and liver harvested after short-term insulin stimulation. Akt2 assays were performed according to methods described previously (25, 43–45). The primary antibody used for experiments was rabbit polyclonal IgG. Antibodies for Akt2 were obtained from Upstate (Charlottesville, VA). For PKC membrane translocation, 50 μg of crude membrane and cytosol protein extracts were resolved by SDS/PAGE by using 8% gel and electroblotted onto PVDF membrane (DuPont, Wilmington, DE) by using a semidry transfer cell (Bio-Rad, Hercules, CA). The membrane was then blocked for 2 h at room temperature in PBS–Tween (10 mM NaH_2PO_4/80 mM Na_2HPO_4/0.145 mM NaCl/0.1% Tween 20, pH 7.4) containing 5% (wt/vol) nonfat dried milk, washed twice, and then incubated overnight with rabbit anti-peptide antibody against PKCε and PKCθ (Santa Cruz Biotechnology, Santa Cruz, CA) diluted 1:100 in rinsing solution. After further washings, membranes were incubated with horseradish peroxidase-conjugated IgG fraction of goat anti-rabbit IgG (Bio-Rad), diluted 1:5,000 in PBS–Tween for 2 h. Membrane translocation of PKCε and PKCθ was expressed as the ratio of membrane bands over cytosol bands (arbitrary units).

Tissue Lipid Measurement. The solid-phase extraction and purification of medium, long-chain, and very long-chain fatty acyl–CoAs

from liver and muscle have been described previously (46, 47). After purification, fatty acyl–CoA fractions were dissolved in methanol/H_2O (1:1; vol/vol) and subjected to liquid chromatography/tandem MS analysis. A turbo ion spray source was interfaced with an API 4000 tandem mass spectrometer (Applied Biosystems, Foster City, CA) in conjunction with two 200 Series micropumps and a 200 Series autosampler (PerkinElmer). The diacylglycerol and ceramide extraction and analysis were performed as described previously (24, 26). Total diacylglycerol and ceramide contents are expressed as the sum of individual species. Tissue triglyceride was extracted by using the Bligh and Dyer method (46) and measured by using a DCL Triglyceride Reagent (Diagnostic Chemicals Ltd., Oxford, CT).

AMPK Activity Assays. The extensor digitorum longus and tibialis anterior muscles were freeze clamped *in situ*. Skeletal muscle samples were kept in liquid nitrogen until analyzed. Muscles were ground with a mortar and pestle and mixed with 1 ml of lysis buffer [50 mM Tris·HCl buffer (pH 7.5 at 4°C)/50 mM NaF/5 mM sodium pyrophosphate/1 mM EDTA/1 mM EGTA/1 mM DTT/1 mM benzamidine/1 mM PMSF/glycerol (10% vol/vol)/Triton X-100 (1% vol/vol)]. Homogenates were spun at 20,800 × *g* for 10 min at 4°C, and protein concentrations were determined. AMPK-α_2 was immunoprecipitated overnight from cell lysates containing 1 mg of protein by using 1 μl of AMPK-α_2 antibody (Santa Cruz Biotechnology). Skeletal muscle AMPK-α_2 activity was determined by following the incorporation of [^{32}P]ATP into a synthetic peptide containing the AMARA sequence on the following day.

Data Analysis and Presentation of Results. All results are expressed as means ± SEM of *n* observations. Statistical differences between the means were assessed by Student's *t* test.

We thank Xiaoxian Ma and Mario Kahn for expert technical assistance with the studies. This work was supported by grants from the Hefni Technical Training Foundation and by National Institutes of Health Grants GM-63115 (to S.J.W.) and R01 DK-40936, U24 DK-76169, and P30 DK-45735 (to G.I.S.). G.I.S. is an investigator of The Howard Hughes Medical Institute and is the recipient of a Distinguished Clinical Investigator Award from the American Diabetes Association. D.B.S. is supported by the Wellcome Traust.

1. Wakil SJ, Stoops JK, Joshi VC (1983) *Annu Rev Biochem* 52:537–579.
2. Munday MR, Hemingway CJ (1999) *Adv Enzyme Regul* 39:205–234.
3. Munday MR (2002) *Biochem Soc Trans* 30:1059–1064.
4. McGarry JD, Brown NF (1997) *Eur J Biochem* 244:1–14.
5. Abu-Elheiga L, Matzuk MM, Abo-Hashema KA, Wakil SJ (2001) *Science* 291:2613–2616.
6. Abu-Elheiga L, Matzuk MM, Kordari P, Oh W, Shaikenov T, Gu Z, Wakil SJ (2005) *Proc Natl Acad Sci USA* 102:12011–12016.
7. Mao J, Chirala SS, Wakil SJ (2003) *Proc Natl Acad Sci USA* 100:7515–7520.
8. Lee JJ, Moon YA, Ha JH, Yoon DJ, Ahn YH, Kim KS (2001) *J Biol Chem* 276:2576–2585.
9. Hardie DG (1989) *Prog Lipid Res* 28:117–146.
10. Kim KH, Lopez-Casillas F, Bai DH, Luo X, Pape ME (1989) *FASEB J* 3:2250–2256.
11. Thampy KG, Wakil SJ (1988) *J Biol Chem* 263:6447–6453.
12. Abu-Elheiga L, Oh W, Kordari P, Wakil SJ (2003) *Proc Natl Acad Sci USA* 100:10207–10212.
13. Oh W, Abu-Elheiga L, Kordari P, Gu Z, Shaikenov T, Chirala SS, Wakil SJ (2005) *Proc Natl Acad Sci USA* 102:1384–1389.
14. Unger RH (1995) *Diabetes* 44:863–870.
15. Pan DA, Lillioja S, Kriketos AD, Milner MR, Baur LA, Bogardus C, Jenkins AB, Storlien LH (1997) *Diabetes* 46:983–988.
16. Krssak M, Falk Petersen K, Dresner A, DiPietro L, Vogel SM, Rothman DL, Roden M, Shulman GI (1999) *Diabetologia* 42:113–116.
17. Shulman GI (2000) *J Clin Invest* 106:171–176.
18. Randle PJ, Garland PB, Hales CN, Newsholme EA (1963) *Lancet* 1:785–789.
19. Randle PJ, Garland PB, Newsholme EA, Hales CN (1965) *Ann NY Acad Sci* 131:324–333.
20. Wolfgang MJ, Lane MD (2006) *J Biol Chem* 281:37265–37269.
21. Choi CS, Fillmore JJ, Kim JK, Liu ZX, Kim S, Collier EF, Kulkarni A, Distefano A, Hwang YJ, Kahn M, *et al.* (2007) *J Clin Invest* 117:1995–2003.
22. Samuel VT, Choi CS, Phillips TG, Romanelli AJ, Geisler JG, Bhanot S, McKay R, Monia B, Shutter JR, Lindberg RA, *et al.* (2006) *Diabetes* 55:2042–2050.
23. Griffin ME, Marcucci MJ, Cline GW, Bell K, Barucci N, Lee D, Goodyear LJ, Kraegen EW, White MF, Shulman GI (1999) *Diabetes* 48:1270–1274.
24. Yu C, Chen Y, Cline GW, Zhang D, Zong H, Wang Y, Bergeron R, Kim JK, Cushman SW, Cooney GJ, *et al.* (2002) *J Biol Chem* 277:50230–50236.
25. Samuel VT, Liu ZX, Qu X, Elder BD, Bilz S, Befroy D, Romanelli AJ, Shulman GI (2004) *J Biol Chem* 279:32345–32353.
26. Neschen S, Morino K, Hammond LE, Zhang D, Liu ZX, Romanelli AJ, Cline GW, Pongratz RL, Zhang XM, Choi CS, *et al.* (2005) *Cell Metab* 2:55–65.
27. Samuel VT, Liu ZX, Wang A, Beddow SA, Geisler JG, Kahn M, Zhang XM, Monia BP, Bhanot S, Shulman GI (2007) *J Clin Invest* 117:739–745.
28. Savage DB, Choi CS, Samuel VT, Liu ZX, Zhang D, Wang A, Zhang XM, Cline GW, Yu XX, Geisler JG, *et al.* (2006) *J Clin Invest* 116:817–824.
29. Summers SA, Nelson DH (2005) *Diabetes* 54:591–602.
30. Holland WL, Brozinick JT, Wang LP, Hawkins ED, Sargent KM, Liu Y, Narra K, Hoehn KL, Knotts TA, Siesky A, *et al.* (2007) *Cell Metab* 5:167–179.
31. Friedman JM (2002) *Nutr Rev* 60:S1–S14.
32. Shi H, Tzameli I, Bjorbaek C, Flier JS (2004) *J Biol Chem* 279:34733–34740.
33. Steppan CM, Bailey ST, Bhat S, Brown EJ, Banerjee RR, Wright CM, Patel HR, Ahima RS, Lazar MA (2001) *Nature* 409:307–312.
34. Lazar MA (2005) *Science* 307:373–375.
35. Hennes MM, Dua A, Kissebah AH (1997) *Diabetes* 46:57–62.
36. Iacopetta B, Carpentier JL, Pozzan T, Lew DP, Gorden P, Orci L (1986) *J Cell Biol* 103:851–856.
37. Meistas MT, Margolis S, Kowarski AA (1983) *Am J Physiol* 245:E155–E159.
38. Jones CN, Abbasi F, Carantoni M, Polonsky KS, Reaven GM (2000) *Am J Physiol* 278:E501–E508.
39. Savage DB, Petersen KF, Shulman GI (2007) *Physiol Rev* 87:507–520.
40. Harwood HJ, Jr (2005) *Expert Opin Ther Targets* 9:267–281.
41. Youn JH, Buchanan TA (1993) *Diabetes* 42:757–763.
42. Rossetti L, Giaccari A (1990) *J Clin Invest* 85:1785–1792.
43. Alessi DR, Andjelkovic M, Caudwell B, Cron P, Morrice N, Cohen P, Hemmings BA (1996) *EMBO J* 15:6541–6551.
44. Folli F, Saad MJ, Backer JM, Kahn CR (1992) *J Biol Chem* 267:22171–22177.
45. Qu X, Seale JP, Donnelly R (1999) *J Endocrinol* 162:207–214.
46. Bligh EG, Dyer WJ (1959) *Can J Biochem Physiol* 37:911–917.
47. Neschen S, Moore I, Regittrig W, Yu CL, Wang Y, Pypaert M, Petersen KF, Shulman GI (2002) *Am J Physiol* 282:E395–E401.